Title

EVALUATING LIQUEFACTION AND LATERAL SPREADING IN INTERBEDDED SAND, SILT AND CLAY DEPOSITS USING THE CONE PENETROMETER

Journal

AUSTRALIAN GEOMECHANICS JOURNAL, 50(4)

ISSN

0818-9110

Authors

Boulanger, Ross W
Moug, Diane M
Munter, Sean K
et al.

Publication Date

2016

Peer reviewed

EVALUATING LIQUEFACTION AND LATERAL SPREADING IN INTERBEDDED SAND, SILT AND CLAY DEPOSITS USING THE CONE PENETROMETER

Ross W. Boulanger, Diane M. Moug, Sean K. Munter , Adam B. Price and Jason T. DeJong
Department of Civil & Environmental Engineering, University of California at Davis, Davis, CA, USA

ABSTRACT

Current procedures for evaluating potential earthquake-induced liquefaction and lateral spreading appear to have a tendency to over-predict liquefaction effects in interbedded sand, silt, and clay deposits. Possible reasons for over-prediction of liquefaction effects are discussed, and investigations regarding some factors pertinent to use of the cone penetrometer are described. An axisymmetric direct cone penetration model is presented for use with the MIT-S1 constitutive model to explore cone penetration processes in a range of soil types; current efforts are focused on validating this new direct cone penetration model, beginning with simulations of cone penetration in soft clay. The relationship between cyclic strength and cone penetration resistance in non-plastic and low-plasticity fine-grained soils is examined by relating cyclic strengths from laboratory tests to cone penetration resistances from simulations. The performance of a site underlain by interbedded soils along the Çark canal during the 1999 M=7.5 Kocaeli earthquake is analysed using one-dimensional lateral displacement index procedures and two-dimensional nonlinear deformation analyses with spatially correlated stochastic models to illustrate how several factors can contribute to an over-prediction of liquefaction effects. Future research needs and directions for improving the ability to evaluate liquefaction effects in interbedded sand, silt, and clay deposits are discussed.

1 INTRODUCTION

Case histories have shown that the engineering procedures currently used in the US and other countries to evaluate potential earthquake-induced liquefaction and lateral spreading appear to have a tendency to over-predict liquefaction effects in interbedded sand, silt, and clay deposits. For example, this was observed in the Gainsborough Reserve and Riccarton areas of Christchurch, New Zealand, where minimal damage occurred but various engineering analyses predict that at least one of the earthquakes in the 2010-2011 Canterbury Earthquake Sequence (CES) should have caused significant ground surface damage due to liquefaction (e.g., Beyzaei *et al*., 2015, Stringer *et al.,* 2015, van Ballegooy *et al.,*. 2014, 2015). Other examples include a site along the Çark Canal in Turkey during the 1999 M=7.5 Kocaeli earthquake (Youd *et al*., 2009) and sites in Taiwan during the 1999 M=7.6 Chi-Chi earthquake (e.g., Chu *et al*., 2007 and 2008).

The apparent tendency of current liquefaction evaluation procedures to over-predict liquefaction effects for interbedded sand, silt, and clay deposits, while conservative, can have large economic implications. For example, it is common to compute a potential for tens of cm of lateral displacement or a few cm of settlement in such deposits, which may lead to potentially unnecessary and expensive ground improvement or structural strengthening efforts.

The purpose of this paper is to discuss possible reasons for over-prediction of earthquake-induced liquefaction effects in interbedded sand, silt and clay deposits and describe results from three research projects regarding factors pertinent to use of the cone penetrometer for liquefaction evaluations. Possible factors contributing to an over-prediction of liquefaction effects in different situations are reviewed first. An axisymmetric direct cone penetration model is presented for use with the MIT-S1 constitutive model to explore cone penetration processes in a range of soil types, including intermediate soils (e.g., silty/clayey sands or sandy/clayey silts) which are often present in interbedded soil deposits. Current work toward validating this direct cone penetration model is illustrated by simulations of penetration resistance in Boston Blue clay. The relationship between cyclic strength and cone penetration resistance in non-plastic and low-plasticity fine-grained soils is then examined by relating cyclic strengths from laboratory tests to cone penetration resistances from simulations. Lastly, the performance of a site underlain by interbedded soils along the Çark canal during the 1999 M=7.5 Kocaeli earthquake is analyzed using one-dimensional (1-D) lateral displacement index (LDI) procedures and nonlinear deformation analyses (NDAs) with spatially correlated stochastic profiles to illustrate how several factors contributed to over-prediction of liquefaction effects at the site. Future research needs and directions for improving the ability to evaluate liquefaction effects in interbedded sand, silt, and clay deposits are discussed.

Table 1: Factors affecting prediction of liquefaction effects in interbedded soil deposits

Factor	Role
Limitations in site characterization tools and procedures	
Interface transitions	Penetration resistance (e.g., q_t) in sand is reduced near interfaces with clays or silts. I_c values increase in the sandy soils and decrease in the clays/silts near the interface.
Thin layer effects	Penetration resistance (e.g., q_t) reduced throughout sand layers less than about 1 m thick (with clays/silts on either side of the layer).
Graded bedding	*In situ* tests measurements may not differentiate between material transitions that occur across distinct interfaces (e.g., erosional contacts) and material transitions that are gradual (e.g., beds with normal or reverse grading, or bed series in fining-upward or coarsening-upward patterns). Transition and thin layer effects in interbedded soils with graded bedding are not well understood.
Continuity of lenses	Large horizontal spacing of explorations may not enable the lateral continuity of weak or liquefiable layers to be evaluated or quantified.
Saturation	Presumption of 100% saturation below the groundwater table may underestimate cyclic strengths for partially saturated zones.
Limitations in correlations for liquefaction triggering or consequences	
Triggering correlations	Triggering correlations are not well constrained for intermediate soils with certain FC and PI combinations; CRR likely underestimated if treated as sand-like, and overestimated if treated as clay-like. Effects of age, stress & strain history, K_o, and cementation not explicitly accounted for.
Strain correlations	Correlations for estimating shear and volumetric strains have been developed primarily from data for sands or clays; the applicability of these correlations for intermediate soils is uncertain.
Limitations from analysis approaches and neglected mechanisms	
Spatial variability	The assumption that liquefiable layers are laterally continuous can contribute to over-estimation of potential liquefaction effects. Composite strength from nonliquefied and liquefied zones may limit deformations.
Thick crust layers	Thick crust layers can reduce surface manifestations of liquefaction at depth in areas without lateral spreading.
Dynamic response	Liquefaction of loose layers in one depth interval may reduce seismic demand on soils in other depth intervals.
Geometry & scale	The 2D or 3D scale of a deformation mechanism affects the dynamic response and role of spatial variability.
Diffusion	Seepage driven by excess pore pressures may increase or decrease ground deformations depending on stratigraphy, permeability contrasts, geometry, seismic loading, and other factors.

2 REVIEW OF CONTRIBUTING FACTORS

The potential for current liquefaction evaluation procedures to over-predict liquefaction effects in interbedded sand, silt and clay deposits stems from several contributing factors, each of which can be important in different situations and depend on the type of analysis method employed. Possible factors contributing to over-predictions in different situations

are listed in Table 1 and grouped into those factors associated with: (1) limitations in site characterisation tools and procedures, (2) limitations in liquefaction triggering or consequence correlations, and (3) limitations from analysis approaches and neglected mechanisms. The first three factors listed under site characterisation tools in Table 1 are described in relation to the cone penetrometer, but analogous issues exist with all in situ testing methods. The next three subsections focus on a subset of factors that are related to use of the cone penetrometer or important to the Çark canal case history. The last subsection provides a more concise review of the other contributing factors.

2.1 SPATIAL RESOLUTION OF CONE MEASUREMENTS

The spatial resolution of cone tip resistance (q_t) and sleeve friction (f_s) measurements as indicators of soil properties is limited by the physical volume of soil around a cone tip that influences these measurements. Measurements of q_t are generally influenced by soils within about 10 to 30 cone diameters around the cone tip, which corresponds to influence zones ranging from about 35 to 130 cm thick for standard 10 cm^2 and 15 cm^2 cones. Measurements of f_s have similar zones of influence because they are influenced by the normal stresses on the friction sleeve (which are related to q_t) and represent an integration of shear stress along the typically 13.4 to 16.4 cm long sleeve. Values of q_t and f_s therefore depend on the sequence and properties of all soils within the zone of influence, which can greatly complicate (and often obscure) the ability to relate q_t and f_s to soil properties at a specific point.

The zone of physical influence around a cone tip is essentially a spatial low-pass variable filter on the q_t and f_s measurements that would have been obtained if they were true point measurements (i.e., a negligible zone of influence). This spatial filtering limits the resolution with which sharp transitions in soil properties can be determined or distinguished from gradual transitions in soil properties (e.g., Frost *et al*., 2006). For example, the values of q_t and f_s measured near a clay-sand interface will smoothly transition from values representative of those for the clay to those for the sand, as illustrated schematically by case 1 in Figure 1. This smooth transition in q_t and f_s values, if interpreted literally on a point-by-point basis, leads to erroneous soil classifications and property estimates in the transition zone. For thin sand seams embedded in clay or plastic silt deposits, the transition zones for the upper and lower interfaces can overlap, which results in q_t values at the middle of the sand seam [$(q_t)_{thin}$ in Fig. 1] that under-predict the sand's true relative density [i.e., as represented by q_t^* in Figure 1]. The difference between $(q_t)_{thin}$ and q_t^* increases as the sand layer thickness decreases, as illustrated by cases 2 and 3 in Figure 1.

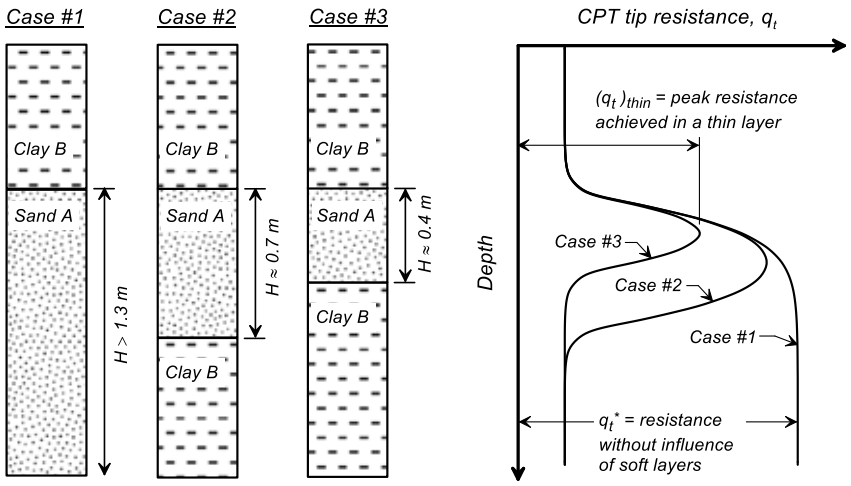

Figure 1: Influence of clay-sand interfaces and sand layer thickness on cone penetration resistance (modified from Robertson and Fear, 1995; after Idriss and Boulanger, 2008).

Limitations in the spatial resolution of property estimates from cone penetrometer data in thin lenses or at interfaces between soils of strongly different properties are well recognized in the literature (e.g., Mayne, 2007). Thin-layer correction procedures have been developed to adjust q_t values from the middle of a thin layer to those that would be measured in a thick layer of the same sand; i.e., $q_t^* = K_H (q_t)_{thin}$, where K_H is a thin-layer correction factor. The thin-layer correction factors shown in Figure 2, for example, include the relationship recommended for liquefaction evaluations at a 1997/98 NCEER workshop (Youd *et al*., 2001). In addition, procedures to account for transition effects at sand-clay interfaces have been developed and implemented in commercially available software for evaluating liquefaction effects (e.g., GeoLogismiki, 2016).

A consistent theoretical and empirical understanding of cone penetration across interfaces or thin layers is lacking, however. For example, the thin-layer correction relationship recommended by Youd *et al*. (2001) based on limited field

data falls below those produced by elastic solutions (Vreugdenhil *et al*., 1994; Robertson & Fear, 1995) as shown in Figure 2. Past experimental studies of cone penetration in layered soils have included tests with sands of different types and relative densities (e.g., Mo *et al*., 2013, 2015; Silva & Bolton, 2004; Canou, 1989 and Foray & Pautre, 1988 as reported in Vreugdenhil *et al.*, 1994). The results show transitions in q_t values over intervals of about 4 to 5 cone diameters, depending on the layer sequence and strength contrasts. Simulations of cone penetration in two layer systems by Van den Berg *et al*. (1996) indicate that when a cone passes from sand into soft clay, the q_t in the sand is influenced when the cone is within about 3 cone diameters of the interface, and when a cone passes from soft clay into sand, it takes about 4 cone diameters of penetration into the sand for the full q_t to develop. Simulations of cone penetration in multi-layered clays by Walker & Yu (2010) show that when a cone passes from a stronger layer to a weaker layer, the q_t is significantly influenced to a distance of about 2 or 3 cone diameters on either side of the interface, whereas when the cone passes from a weaker layer to a stronger layer, the q_t rises more abruptly. The transition interval thicknesses obtained in the above experiments and simulations would suggest that thin-layer effects should be smaller than indicated by the empirical thin-layer correction factors recommended in Youd *et al*. (2001) (Figure 2). It is likely that additional experimental data, numerical simulations and field studies will be required to develop a consistent understanding of thin-layer effects for sand lenses interbedded with softer fine-grained sediments.

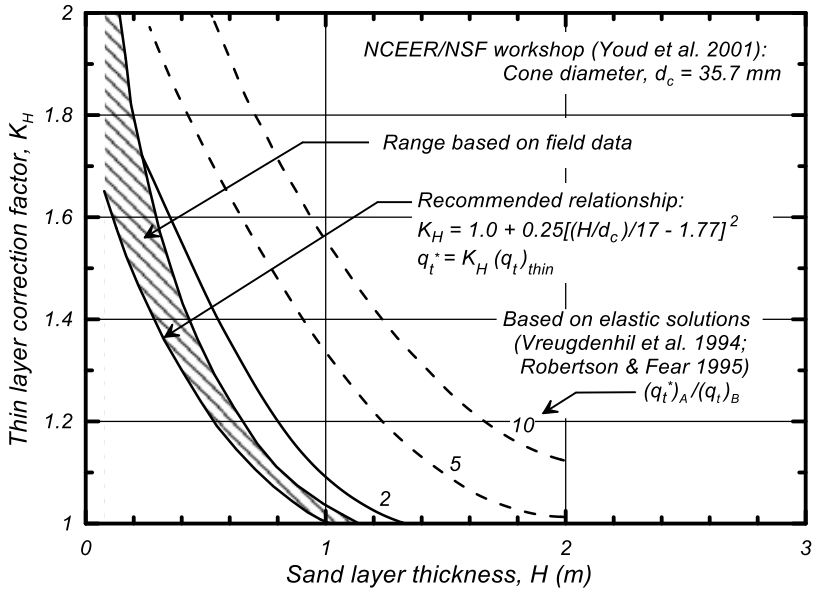

Figure 2: Thin layer correction factors for determining equivalent thick-layer cone tip resistance (modified from Youd *et al*., 2001 after Idriss and Boulanger, 2008).

The influence of graded bedding on interface transition and thin-layer effects is another issue that needs to be addressed (Table 1). Individual beds of sand may exhibit normal grading (upward decrease in grain size) or reverse grading (upward increase in grain size), and series of beds can be arranged in fining-upward or coarsening-upward sequences (Nichols, 2009). Current procedures for evaluating interface transition and thin-layer effects lack guidance on how one should distinguish between interfaces where soil properties transition gradually (e.g., a fining-upward sequence) versus sharply (e.g., an abrupt transition from sand to clay at an erosional contact). Measurements of q_t and f_s cannot be expected to differentiate between a sharp transition and a gradual transition that occurs over a length scale that is similar to, or smaller than, the zone of physical influence around the cone tip. Characterising graded bedding at these smaller scales may instead require supplemental information, such as continuous core samples from the same deposit. Regardless, the currently available transition and thin-layer correction procedures were developed for abrupt soil transitions and the potential impacts of applying them to deposits with gradual transitions have not been adequately examined.

The problem in practice is that using cone penetrometer data in interbedded deposits without transition and thin-layer corrections has the potential to significantly under-estimate the available resistance to liquefaction triggering or deformation. These effects are illustrated in Figure 3 for an idealized analysis of a thin clean sand layer embedded in a clay deposit at a depth where the initial vertical effective stress (σ'_{vo}) is 100 kPa. The normalized tip resistance ($q_{tN} = q_t/P_a$ where P_a = atmospheric pressure) in the clay is 20. The sand layer is characterized by the "true" value of q_{tN} that it would have had if the layer were thick. The value of q_{tN} "measured" at the middle of the sand layer is the "true" q_{tN} divided by the thin-layer correction factor K_H based on field data from Youd *et al*. (2001), as shown in Figure 2. The "measured" q_{tN} is assumed to transition linearly from the clay value to the mid-sand-layer value over a transition interval of either 15 cm (blue lines) or 30 cm (red lines), or just half the sand layer thickness if the sand layer is thinner

than twice the transition interval thickness. The "measured" sleeve friction is assumed to produce normalized tip resistance (Q) and sleeve friction ratio (F) values that plot in the middle of the normally consolidated zone on the soil behaviour type chart by Robertson (1990). The cyclic resistance ratio (CRR) for M=7.5 and σ'_{vo} = 1 atm was computed using the liquefaction triggering correlation by Boulanger & Idriss (2015); this calculation based on the "measured" CPT data includes the apparent increase in fines content as the sand layer thickness decreases (i.e., Q decreases and the soil behaviour type index I_c increases). Lastly, the average CRR across the sand layer was computed and plotted versus the sand layer thickness in Figure 3 for various "true" q_{t1N} values. The results in Figure 3 illustrate how the use of CPT data without transition and thin-layer corrections can significantly under-predict the CRR of dense sand lenses less than about 1 m thick and cannot distinguish between loose or dense conditions for sand lenses less than about 0.3 m thick. Ideally, transition and thin-layer corrections would remove this source of potential bias, but the details of their application are subjective in practice (e.g., the issue of graded bedding) and difficult to automate. For this reason, these corrections are not uniformly applied or relied upon.

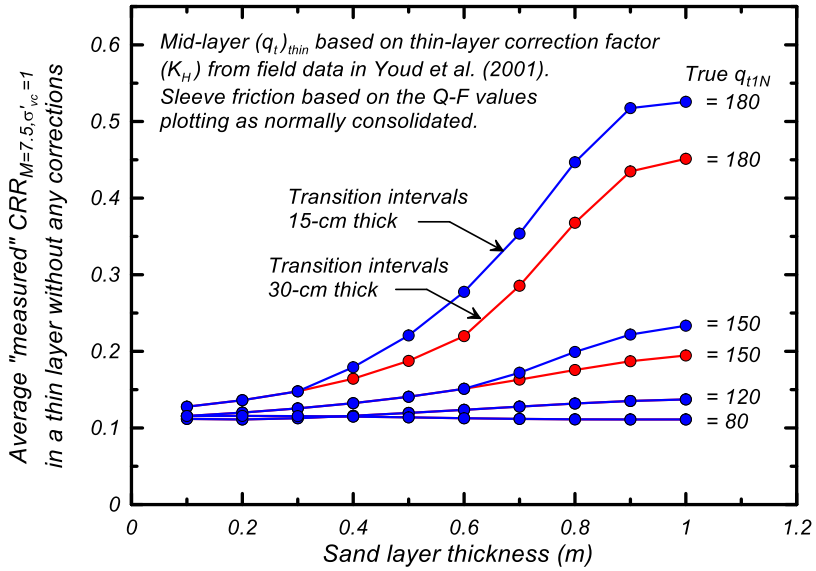

Figure 3: Idealized example illustrating the underestimation of CRR for a thin sand layer embedded between clay layers if transition and thin-layer corrections are not applied.

2.2 INTERMEDIATE SOIL TYPES

Current liquefaction triggering correlations (e.g., Robertson & Wride, 1998; Moss *et al*., 2006; Boulanger & Idriss, 2015) have some of their greatest differences in silty sands, sandy silts and silts of low-plasticity. These differences are not surprising because the triggering correlations are not well constrained by the limited number of case histories involving intermediate soil types and thus their differences also stem from differences in their functional forms. Recent research has shown that q_t in low-plasticity fine-grained soils can vary strongly with small changes in clay content [or plasticity index (PI)], and this has a strong effect on the correlation to cyclic strength for soils with high percentages of fines that are either non-plastic or of low plasticity (say PI < ~ 5). Current liquefaction triggering procedures do not have theoretical bases or sufficient field data for confidently constraining these correlations across the full range of possible fines content (FC) and PI combinations.

Procedures for evaluating cyclic strengths have tended to be either well suited for sand-like soils or well suited for clay-like soils. For sand-like soils, concerns with the effects of sampling disturbance have led to an emphasis on case history based liquefaction triggering correlations using CPT, SPT or shear wave velocity (V_s) data. For clay-like soils, the ability to sample and test with reasonable confidence has led to procedures that are similar to those used to evaluate monotonic undrained shear strengths. An artifact of these two different approaches has been sharp jumps in the estimated cyclic strength when the soil classification toggles across a classification of clay-like versus sand-like. These sharp jumps in CRR values were illustrated by Robertson (2009) as contours on a soil behaviour type chart (Figure 4).

Similarly, correlations for estimating earthquake-induced shear strains or post-shaking reconsolidation strains have been developed primarily from laboratory test data for either sands or clays. The extension of these correlations to intermediate soils has not been systematically examined, and is another source of potential bias in evaluating liquefaction consequences (Table 1).

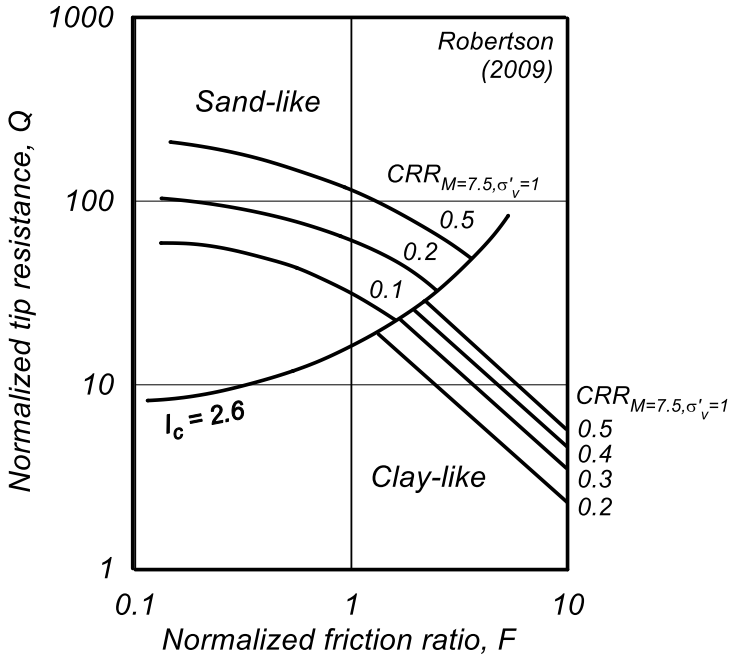

Figure 4: Contours of $CRR_{M=7.5,\sigma'=1}$ for sand-like and clay-like soils based on the procedures by Robertson and Wride, (1998) for sand-like soils and by Boulanger and Idriss (2007) for clay-like soils (after Robertson, 2009).

The fundamental basis for cone penetration resistance to correlate with cyclic strengths also warrants discussion. Consider the schematic in Figure 5 showing critical state lines, initial conditions, and stress paths for a point near the cone tip as it penetrates either medium-dense sand or normally consolidated clay. The monotonic loading imposed by cone penetration produces an undrained stress path that moves to the left in the normally consolidated clay and a drained path that moves to the right in the medium-dense sand. The path for the medium-dense sand moves down and to the right because the sand is much less compressible under monotonic loading (as represented by a flatter critical state line at lower stresses) and is initially dense of critical state, which together lead to large mean stresses near the cone tip during drained penetration. The path for the medium-dense sand under seismic loading, however, would potentially be to the left if saturated and largely undrained during the seismic loading. The path for seismic loading may move to the left because the sand can accumulate net plastic volumetric contractive strains during reversed cyclic loading, which causes a loss of effective stress for undrained conditions. Thus, the stress path followed by sand during cone penetration is not the same as that for seismic loading. The greater compressibility of clay relative to sand and the undrained conditions during cone penetration in clay (versus drained in sand) result in much lower cone penetration resistances, even if the clay is heavily over-consolidated and has a large cyclic strength. For sand or clay, cyclic strength correlates with cone penetration resistance because variations in fundamental properties or soil characteristics that tend to increase cone penetration resistance also tend to increase cyclic strength, and vice versa (e.g., state, compressibility, stress history, age, and cementation). The effects of variations in the fundamental properties or soil characteristics on cyclic strength and cone penetration resistance are nonetheless unlikely to be identical, which is one source of dispersion in the resulting correlations for either sand or clay. At the same time, the general differences in fundamental properties for sand versus clay are sufficiently large that distinctly different cyclic strength correlations have been developed for these two soil types. The subsequent application of these correlations therefore depends strongly on soil characteristics that are currently only accounted for by broad categorisations such as clay-like or sand-like. The generalisation of cyclic strength correlations across intermediate soil types (i.e., from sand to clay) would benefit from a more generalised theoretical framework and may also benefit from independent measures or indices of other soil attributes, such as shear wave velocity, compressibility and permeability.

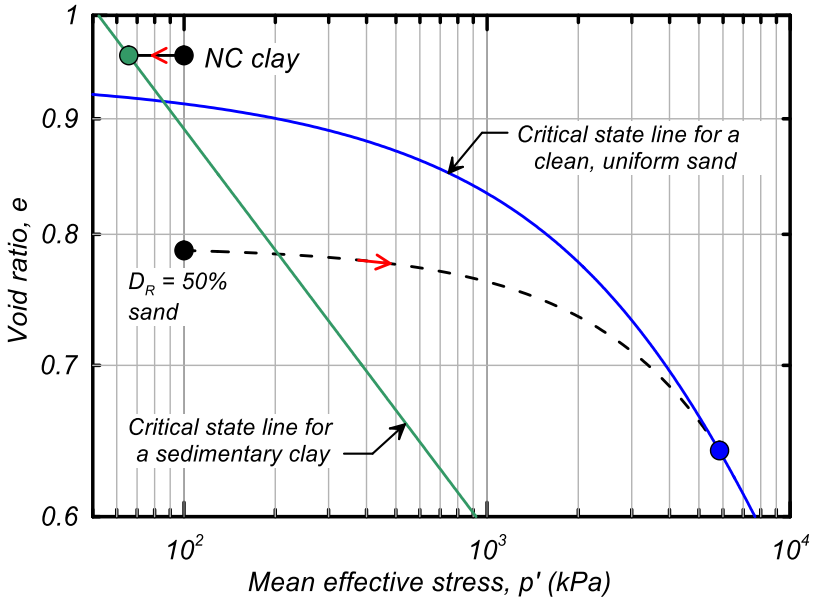

Figure 5: Schematic of loading paths near a penetrating cone in normally consolidated clay (an undrained path) or medium dense sand (a drained path).

2.3 SPATIAL VARIABILITY

Simplifying and ultimately conservative assumptions regarding the lateral continuity and extent of liquefiable lenses within interbedded deposits are explicitly incorporated in some liquefaction evaluation methods and often implicitly invoked in the application of other liquefaction evaluation methods. For example, liquefaction vulnerability indices (LVIs) such as the lateral displacement index (LDI), liquefaction potential index (LPI), liquefaction severity number (LSN), or post-liquefaction reconsolidation settlement ($S_{v\text{-}1D}$) are all commonly computed using data from individual borings or CPT soundings. These calculations are therefore based on the assumption of horizontal layering with infinite lateral extent, such that the results are referred to as 1-D LVIs. Other liquefaction evaluation methods include empirical regression models (e.g., the multiple linear regression models by Youd *et al*., 2002) and Newmark sliding block methods (e.g., Olson & Johnson 2008). In applying these methods, it is common in practice to conservatively assume lateral continuity or connectivity of liquefiable layers across borings and soundings that are often spaced too far apart for the lateral continuity to be properly evaluated.

Limited lateral continuity of liquefiable lenses in interbedded sand, silt and clay deposits has been hypothesized as a possible factor when ground deformations are over-predicted by current liquefaction evaluation procedures. In these cases, it is possible that any potential failure or shear deformation mechanisms must engage both liquefiable and nonliquefiable soils, and that the shear strengths of the nonliquefiable soils are sufficient to reduce ground deformations. Youd *et al*. (2009) concluded this was the case at Çark Canal during the 1999 M=7.5 Kocaeli earthquake, for example. NDAs using stochastic models of interbedded sands and clays in mildly sloping ground demonstrated this is potentially a major factor controlling lateral spreading displacements (Munter *et al*., 2016). More generally, Cubrinovski & Robinson (2015) examined characteristics of lateral spreads in the 2010-11 CES and concluded that small-displacement lateral spreads were associated with thin critical layers that were discontinuous along and away from the river, and that large-displacement lateral spreads of narrow extent were associated with critical layers confined within narrow zones along riverbanks. Their findings illustrate the importance of the scale of the critical layers relative to the scale of the deformation mechanisms.

Methods for systematically evaluating spatial variability in interbedded deposits and accounting for it in liquefaction evaluation procedures are not well developed. Improved guidance on how to systematically account for the influence of spatial variability in estimating vertical settlements and/or lateral spreading in naturally variable deposits is needed.

2.4 OTHER CONTRIBUTING FACTORS

Several other factors, in addition to those discussed above, are considered as likely contributing to why current liquefaction evaluation procedures can sometimes over-predict liquefaction effects in interbedded sand, silt and clay deposits (Table 1). The significance of each factor depends, in part, on the analysis approach being used to evaluate liquefaction effects: e.g., empirical regression models, 1-D LVIs, Newmark sliding block models, or NDAs.

One factor is the role of thick crust layers in reducing surface manifestations of liquefaction in areas without lateral spreading (e.g., Ishihara, 1985). A crust layer that is sufficiently thick relative to the extent and thickness of any liquefied zone can reduce differential surface settlements, ground cracking, and emergence of soil ejecta. This effect can also complicate case history interpretations, especially in distinguishing cases of non-manifestation from cases of non-liquefaction triggering.

Another possible factor is partial saturation of soils within some depth interval below the ground water table, with the partially saturated soils having a greater cyclic resistance than otherwise expected. Soils may be partially saturated because of past water table fluctuations or chemical and biological activity. The greater cyclic strength of a partially saturated zone could result in a thicker crust of nonliquefied materials that could help reduce surface manifestations of liquefaction, as discussed above.

Another possible factor is the influence of liquefaction on the dynamic response of a site, such that liquefaction of looser soils within one depth interval may reduce the dynamic stresses and strains imposed on soils in other depth intervals. Simplified 1-D LVI procedures do not account for these effects and thus will over-predict the potential for lateral displacements in situations where they are significant.

Another factor is that the inter-bedding of sand, silt and clay impedes the diffusion of excess pore water pressures that develop within the liquefiable lenses. In some cases, this impeding of diffusion may reduce deformations relative to those that can develop in thick layers of liquefiable sands where a steady upward flow of pore water may weaken soils near the surface and contribute to deformations. In other cases, this impeding of diffusion may increase deformations if it leads to sufficiently extensive water film formation or localized strength loss (e.g., Kokusho, 2003, Boulanger *et al*., 2014). The potential for impeded diffusion to increase or decrease deformations depends on the stratigraphy, permeability contrasts, geometry, seismic loading and other factors. It is difficult to predict diffusion effects during and after seismic loading even with advanced NDAs, and the empirical data are still insufficient to propose accounting for these effects in any simplified method.

In most cases, it is likely that several of the factors listed in Table 1 will contribute to any observed bias in liquefaction evaluations for interbedded sand, silt and clay deposits. The degree to which each factor contributes will depend on the specific situation and the analysis method employed. For this reason, the systematic evaluation of case histories with due consideration to all contributing factors will be important for developing improved guidance for practice.

3 DIRECT CONE PENETRATION MODEL

Numerical simulations for cone penetration have been performed for sand or clay using direct and indirect axisymmetric models. Direct models simulate penetration with the full cone geometry, whereas indirect models simulate cylindrical or spherical cavity expansion. Indirect models require converting the cavity expansion limit pressure to a cone tip resistance using relationships or procedures that are significantly different for sand versus clay. A direct model is preferable for studying intermediate soils (e.g., silty and clayey sands) because indirect conversion procedures are not available for these soil types.

A direct axisymmetric model for cone penetration in intermediate soils requires a constitutive model that can reasonably approximate a broad range of soil behaviors. A review of the literature (Moug *et al*., 2016) found that direct penetration models have primarily used relatively simple elastic-plastic constitutive models, such as Mohr-Coulomb (e.g., Huang *et al*. 2004; Chai *et al*., 2012); von-Mises (e.g., Walker & Yu, 2006; Liyanapathirana, 2009; Wang *et al*., 2015), Drucker-Prager (e.g., Yi *et al*., 2012) and modified Cam Clay models (e.g., Yu *et al*., 2000; Chai *et al*., 2012; Mahmoodzadeh *et al*., 2014). These types of constitutive models are not general enough to simulate the full range of intermediate soil behaviours.

A direct axisymmetric model for steady state cone penetration using the MIT-S1 constitutive model was therefore developed by Moug *et al*. (2016). The MIT-S1 constitutive model (Pestana & Whittle, 1999), with its generalized, bounding surface formulation, is able to approximate the stress-strain responses of a broad range of soil types. The MIT-S1 model was implemented in the finite difference platform FLAC 7.0 (Itasca, 2011) by Jaeger (2012). The penetration model implemented by Moug *et al*. (2016) uses an Arbitrary Lagrangian Eulerian (ALE) algorithm that couples the large deformation Lagrangian formulation in FLAC with a user-written rezoning algorithm and a user-written second-order Eulerian advection remapping algorithm after Colella (1990). Interface elements between the soil and cone enable the specification of interface friction angles, as opposed to assuming purely rough or purely smooth interfaces. An example mesh for the axisymmetric model and its boundary conditions are shown in Figure 6.

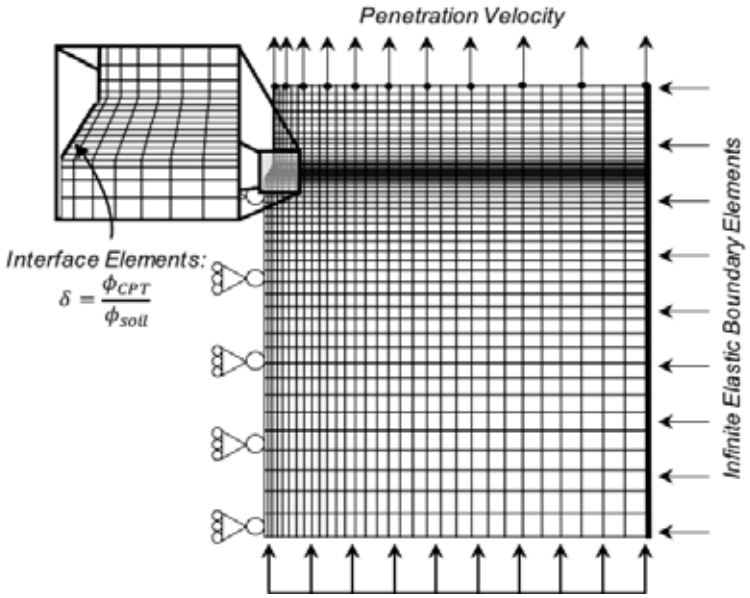

Figure 6: Boundary conditions and mesh for direct axisymmetric penetration model (Moug *et al*., 2016).

The first application of this direct penetration model was an examination of cone penetration in Boston Blue Clay (BBC) using the Mohr-Coulomb (MC), Modified Cam Clay (MCC), and MIT-SI constitutive models. Details are in Moug *et al*. (2016).

Laboratory test results on intact samples (Landon, 2007) and re-sedimented specimens (Ladd & Varallyay, 1965) show that BBC has significant strength anisotropy. The undrained shear strength ratio (s_u/σ'_{vo}) for $CK_{ONC}UC$ loading is about 0.28 and 0.33 for intact and resedimented specimens, respectively. The s_u/σ'_{vo} for $CK_{ONC}UDSS$ and $CK_{ONC}UE$ loading of resedimented specimens decreases to 0.20 and 0.14, respectively.

Only the MIT-S1 model is able to approximate the BBC's strength anisotropy, as illustrated in Figure 7 showing single-element simulations for $CK_{ONC}UC$ and $CK_{ONC}UE$ loading with the three constitutive models calibrated to the same $CK_{ONC}UC$ strength. The MC and MCC models produce the same s_u in extension and compression, whereas the MIT-S1 model is able to simulate a much lower s_u in extension than in compression. The MIT-S1 calibration is presented in Jaeger (2012), which was updated from the calibration in Pestana *et al*. (2002).

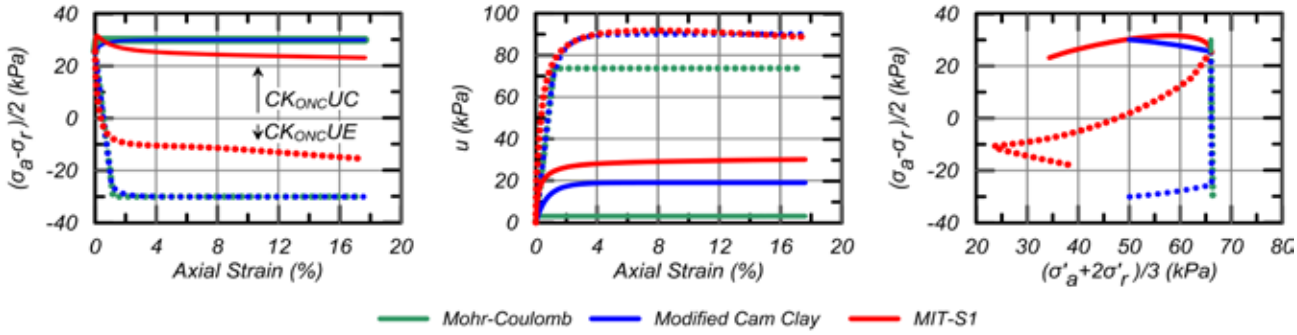

Figure 7: Single element simulations of BBC response in $CK_{ONC}UC$ and $CK_{ONC}UE$ loading using the MC, MCC and MIT-SI constitutive models calibrated to the same $CK_{ONC}UC$ strength (after Moug *et al*., 2016).

The pore pressure and stress path responses for the single-element simulations in Figure 7 illustrate the significant differences in shear-induced pore pressure for the three constitutive models. The MC model, with a friction angle of zero and associative flow, does not develop plastic volumetric strains during deviatoric loading and thus only develops excess pore pressure in response to changes in mean total stress. The MCC model generates greater pore pressures than the MC model for either loading condition because the MCC model does develop plastic volumetric strains once the yield surface has been reached. The MIT-S1 model generates even greater pore pressure for either loading path because its more flexible formulation enabled a calibration that could approximate pore pressures associated with the BBC strength anisotropy.

Cone penetration at a BBC site in Newbury, Massachusetts was then simulated for a depth of 9.6 m where the vertical total stress was 175 kPa, vertical effective stress was 100 kPa, and the over-consolidation ratio (OCR) was about 2.2 (Landon, 2007). The measured q_t at this depth range from 530 to 730 kPa (Landon, 2007). The simulated cone penetration resistances (q_t) were reached by about 5 cone diameters of penetration for all three soil models (Figure 8). Cone tip resistances with the MC and MCC soil models are both about 750 kPa, which is consistent with both models producing essentially the same s_u of 59 kPa for either CK_OUC or CK_OUE loading conditions. The cone bearing factor N_{kt} from these simulations, with their essentially isotropic s_u values, correspond to an $N_{kt,iso}$ of about 9.7.

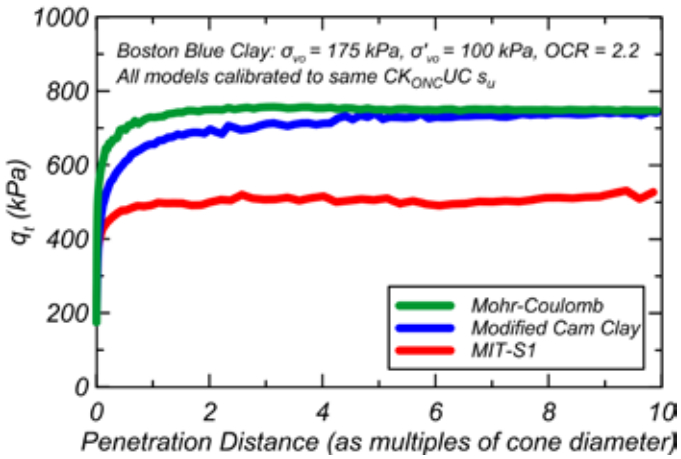

Figure 8: Simulated tip resistance versus penetration distance from wished in-place initial condition. (after Moug *et al*., 2016).

Cone tip resistance with the MIT-S1 model was about 515 kPa, or 31% smaller than with the MC and MCC models. The MIT-S1 model produces a smaller q_t value because its calibration produces smaller s_u values for all but the CK_OUC loading condition; i.e., MIT-S1 with OCR of 2.2 and σ'_{vc} = 100 kPa produces s_u of 54, 36 and 38 kPa for CK_OUC, CK_ODSS and CK_OUE loading conditions respectively. This simulation result thus corresponds to $N_{kt,C}$, $N_{kt,DSS}$ and $N_{kt,E}$ values of 6.3, 9.4 and 8.9, respectively. The cone tip resistance could alternatively be related to the average s_u for these three test types (i.e., 43 kPa for this example) which would correspond to an $N_{kt,ave}$ of 8.0.

The simulated total vertical stress fields around the penetrating cone at 25 cone diameters of penetration are shown in Figure 9 for each soil model. The steady state stress distributions show similar stress values in the cone tip area for MC and MCC models, while total vertical stress is less for the MIT-S1 model. The differences in total vertical stress are consistent with the differences in cone tip resistance for the three models.

Steady state pore pressure fields are presented in Figure 10 for the three constitutive models. There are two components to the pore pressures generated during undrained cone penetration: (1) pore pressure due to a change in total mean stress, and (2) pore pressure due to deviatoric loading. Pore pressures induced by the cone penetration with the MCC model are slightly greater than with the MC model. The total stress fields are similar for the two models because they have similar strengths and therefore produce similar cone tip resistances. The MCC model, however, produces more pore pressure during deviatoric loading as illustrated by the single element simulations in Figure 7.

The steady state pore pressure for the MIT-S1 model shows smaller pore pressures near the cone face, but greater pore pressures for some zones near the cone shaft above the tip. The smaller pore pressures near the cone face are attributed to the MIT-S1 model producing smaller mean total stresses and smaller cone tip resistance because of its lower average strength. The pore pressures near the cone shaft above the tip are larger with MIT-S1 because it produces more pore pressure during deviatoric shearing (as shown by the single element simulations in Figure 7) and the mean total stresses for the three models are not as different in this area.

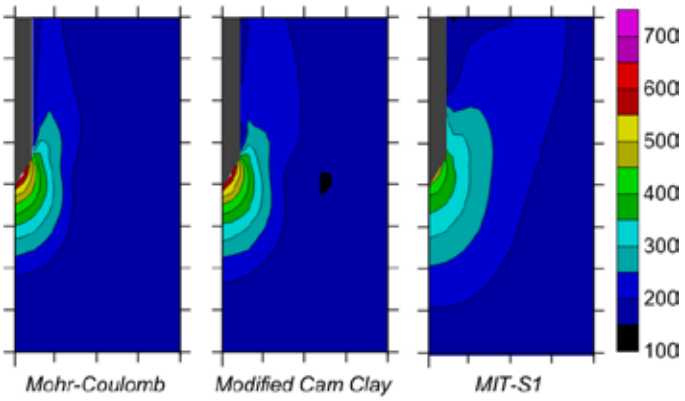

Figure 9: Total vertical stress at 25 cone diameters of penetration in Boston Blue Clay; σ_{vo} =175 kPa prior to penetration (after Moug *et al.,* 2016)

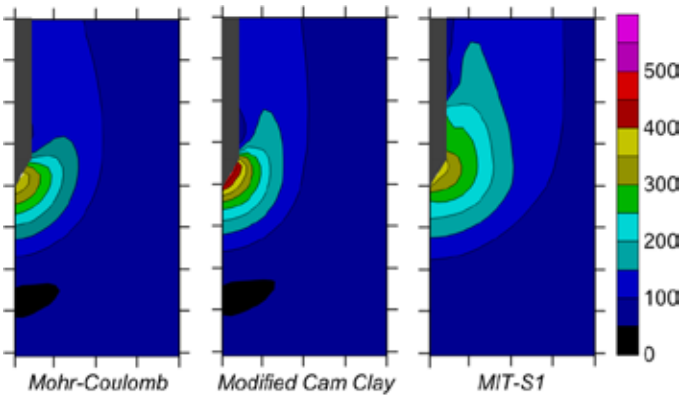

Figure 10: Pore water pressure at 25 cone diameters of penetration in Boston Blue Clay; u_o = 75 kPa prior to penetration. (after Moug *et al*., 2016).

The cone tip resistances for the Newbury site were slightly over-estimated with the MCC and MC models and slightly under-estimated with the MIT-S1 model. The analyses with the MCC and MC models over-predicted q_t because they were calibrated to the stronger $CK_{ONC}UC$ loading condition. The under-prediction obtained with the MIT-S1 model suggests that calibration to resedimented BBC data may have underestimated *in situ* s_u values for some of the loading conditions that develop around the cone. Overall, the reasonable agreement between simulated and measured tip resistances provides a measure of validation for the cone penetration model.

The development of a direct cone penetration model with the MIT-S1 constitutive model was considered an important step for supporting studies of some factors contributing to over-predictions of liquefaction effects in interbedded sand, silt and clay deposits (Table 1). One objective is developing a mechanistic framework for relating CPT data to cyclic behaviours of intermediate soils. Another objective is examining the influence of interface transitions, thin layers, and graded bedding on cone penetrometer measurements. For these objectives, the simulation of cone penetration with realistic constitutive responses is expected to provide improved insights and capabilities.

4 LIQUEFACTION TRIGGERING CORRELATION FOR INTERMEDIATE SOILS

Advancement of CPT based methods for estimating cyclic strengths of intermediate soils requires improvements in our understanding of the properties influencing cone penetration and cyclic loading behaviours. For example, insights have been obtained from studies examining cyclic strength and cone tip resistance in intermediate soils through cyclic lab tests, cone penetration tests in calibration chambers, and numerical simulations of cone penetration (Salgado *et al*., 1997; Carraro *et al*., 2003, Cubrinovski *et al*., 2010; Jaeger, 2012, Kokusho *et al*., 2012; Park & Kim, 2013, DeJong *et al*., 2013).

In this section, initial results are presented for a study relating laboratory measured cyclic strengths to simulated cone tip resistances in mixtures of nonplastic silt and kaolin (Price *et al*., 2015). Non-plastic silica silt and kaolin clay were blended to create soil mixtures with PIs of 0, 6, and 20. The PI = 0 mixture was 100% silica silt, the PI = 6 mixture was 80% silica silt and 20% kaolin clay by dry mass and the PI = 20 mixture was 30% silica silt and 70% kaolin clay.

The monotonic and cyclic loading responses of slurry deposited specimens at different over-consolidation ratios were characterized by undrained monotonic and cyclic direct simple shear (DSS) tests and one-dimensional consolidation tests. The cyclic loading response of normally consolidated specimens of the PI = 0 and PI = 20 mixtures are shown in Figure 11. The cyclic stress ratios required to cause single-amplitude peak shear strains of 3% are plotted versus number of loading cycles in Figure 12 for all three mixtures and OCRs of 1 and 4. Over-consolidation increased the CRR values for all three mixtures, although the increase was greater for the PI = 6 and 20 mixtures than for the PI = 0 soil. The CRR values ranged from 0.10 to 0.14 for the NC specimens and from 0.21 to 0.29 for the OCR = 4 specimens. The observed variation in CRR with mixture PI and OCR is conditional on the three mixtures having been placed by a similar depositional process, while recognizing that they are unavoidably different in all other key characteristics (e.g., initial void ratio, critical state line, compressibility). Comparisons of laboratory strengths obtained on soil mixtures with different characteristics (e.g., fines contents, PIs, OCRs, fabrics) become more valuable if they can instead be expressed conditional on independent test measurements available in practice, such as data from a cone penetrometer.

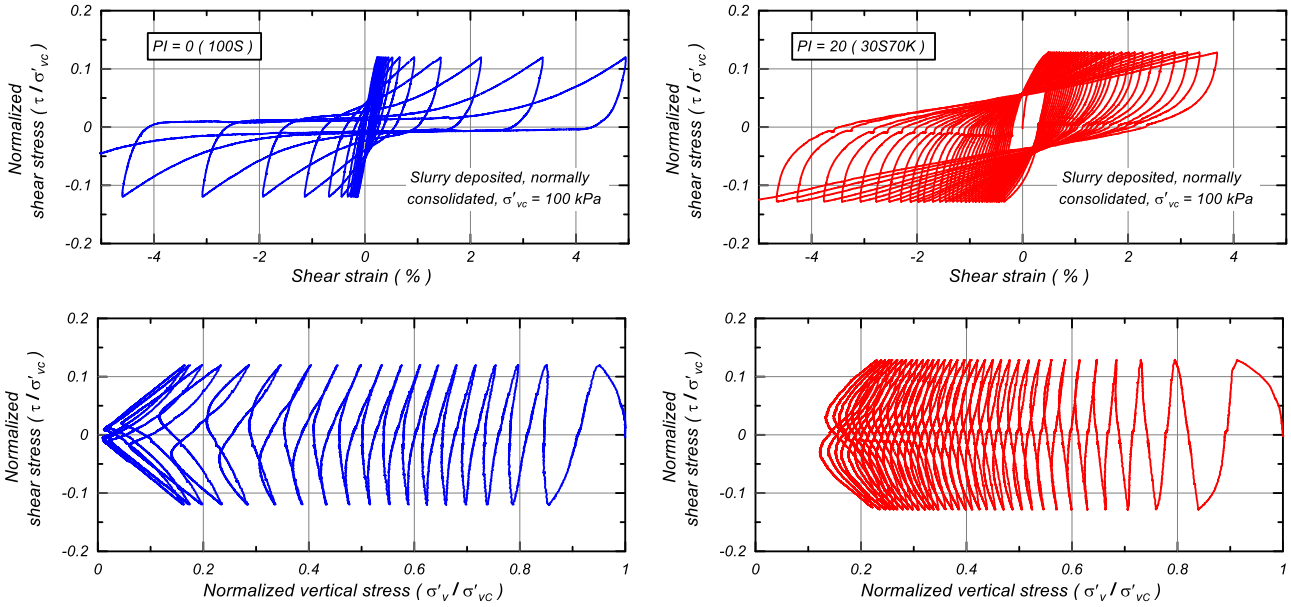

Figure 11: Undrained cyclic direct simple shear test results for normally consolidated, slurry sedimented specimens of PI=0 silt (left side) and PI=20 clayey silt (right side).

Indirect cone penetration analyses were performed in this preliminary work because the direct penetration model described in the previous section was still under development. Cylindrical cavity expansion simulations were performed in FLAC using the MIT-S1 model. The calibrated response of the MIT-S1 model for the three soil mixtures is illustrated in Figure 13 for undrained monotonic DSS loading of normally consolidated specimens. The limit pressures from the cavity expansion analyses were converted to cone tip resistances using the procedure by Leblanc & Randolph (2008), although the appropriateness of this or other conversion procedures for nonplastic and low plasticity silts has not yet been established.

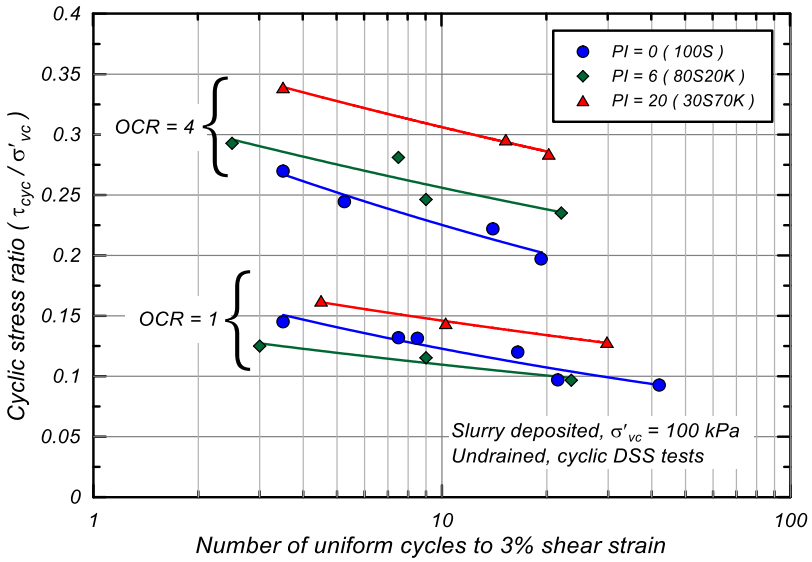

Figure 12: Cyclic stress ratio to 3% single amplitude peak shear strain in undrained cyclic DSS tests on slurry sedimented specimens of PI = 0, 6, and 20 soils at OCRs of 1 and 4 (after Price *et al*., 2015)

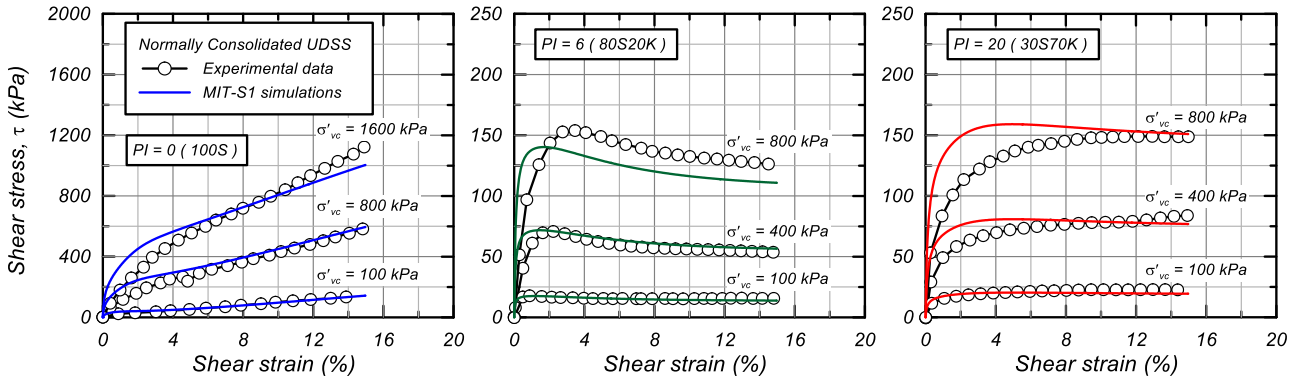

Figure 13: Simulation of undrained monotonic DSS responses for normally consolidated, slurry sedimented specimens of the PI = 0, 6, and 20 soils at different initial consolidation stresses (Price *et al*., 2015).

The laboratory measured cyclic strengths are related to the simulated cone tip resistances in Figure 14 for the three mixtures and σ'_{vc} = 100 kPa. The shaded regions for each mixture indicate the range of tip resistances for drained and undrained conditions. Cone penetration in the field would be expected to range from partially drained for the PI = 0 and 6 soils to largely undrained for the PI = 20 soil based on their measured coefficients of consolidation and established relationships for drainage during cone penetration (e.g., DeJong & Randolph, 2012). The curves relating CRR to tip resistance for the PI = 6 and 20 soils are located much further to the left than the curves for the PI = 0 soil. This leftward shift with a small amount of plasticity is primarily due to the order-of-magnitude smaller tip resistances for the PI = 6 and 20 soils, whereas the CRR values for all three mixtures at any given OCR varied to a lesser extent (Figure 12). The order-of-magnitude smaller tip resistances for the PI = 6 and 20 soils relative to the PI = 0 soil are consistent with their differences in compressibility and initial states (Price *et al*., 2015), as schematically illustrated previously in Figure 5. The results in Figure 14 are consistent with studies showing that the leftward shift in SPT liquefaction triggering correlations with increasing fines content is largely attributable to the effects of the fines on the SPT penetration resistance (e.g., Cubrinovski *et al*., 2010).

Empirical curves of CRR versus tip resistance are also shown in Figure 14 for clays and nonplastic silts at a σ'_{vc} of 100 kPa. The relationships between CRR and undrained tip resistance for the PI = 6 and 20 soils are in reasonable agreement with the empirical curve for ordinary sedimentary clays. The range of CRR versus tip resistance curves for the PI = 0 soil is also in reasonable agreement with its corresponding empirical correlation for nonplastic liquefiable soils (Boulanger & Idriss, 2015). The general agreement between the relationships developed for these PI = 0, 6, and 20 soils and their applicable empirical counterparts is promising in suggesting that the present approach can be used to

further examine the use of CPT tests for estimating cyclic strengths of intermediate soils across a broader range of *in situ* conditions.

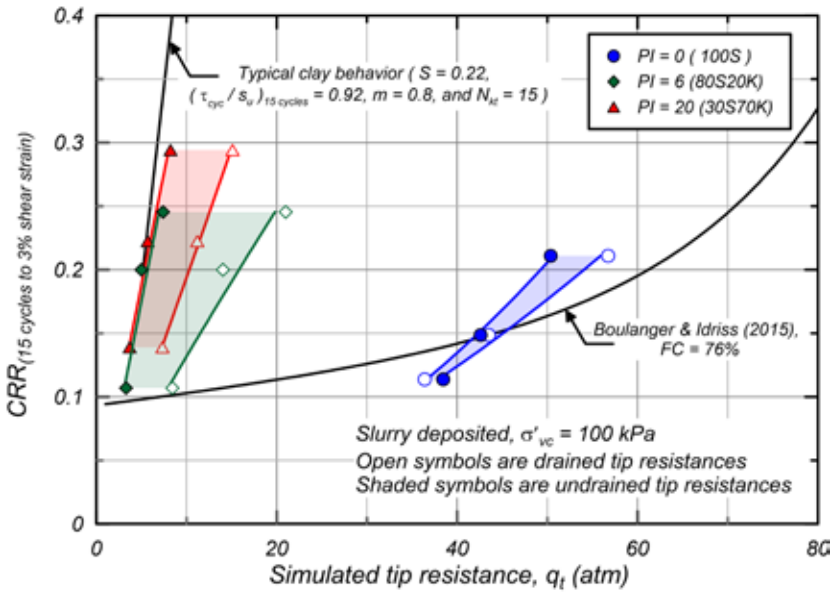

Figure 14: Measured cyclic strength versus simulated cone tip resistance for slurry sedimented PI = 0, 6, and 20 soils at OCR of 1, 2, and 4 (Price *et al*., 2015).

Results from this project are expected to support the refinement of triggering correlations for intermediate soils, which is one potential factor contributing to over-prediction of liquefaction effects in interbedded sand, silt, and clay deposits (Table 1). Future work will include examining additional intermediate soil mixtures, repeating the cone penetration simulations with the direct penetration model described in the previous section and validating select cases with centrifuge model tests. Interpretation of these results will also examine how CPT based relationships may be augmented by independent measurements of the soil's mechanical properties, such as small-strain shear wave velocity or limiting compression behaviour.

5 EVALUATION OF LIQUEFACTION EFFECTS AT ÇARK CANAL

The performance of a site underlain by interbedded soils along the Çark canal in the 1999 M=7.5 Kocaeli earthquake is reexamined to evaluate how different factors can contribute to an over-prediction of liquefaction effects. Lateral spreading displacements are estimated using 1-D LDI procedures and 2-D NDAs with spatially correlated stochastic models. The results of the LDI analyses illustrate the potential importance of transition and thin-layer corrections in CPT based evaluations of liquefaction effects for interbedded sand, silt and clay deposits. The results of the NDA analyses illustrate the additional roles of spatial variability, geometry and nonlinear dynamic response.

The characterization of a section of Çark canal and its performance during the 1999 M=7.5 Kocaeli earthquake was presented by Youd *et al*. (2009). The canal is a channelized segment of the meandering Çark River. The critical stratum for evaluating ground deformations is a fluvial deposit of predominantly clay-like fine-grained sediments with interbedded silty sands, as shown on the cross-section in Figure 15. Five CPT soundings and two borings with SPTs were performed at the site and documented in Youd *et al*. (2000). No lateral spreading damage was observed at the site after the Kocaeli earthquake despite an estimated peak ground acceleration of 0.4 g. Youd *et al*. (2009) showed that current liquefaction susceptibility criteria in combination with a multiple linear regression model greatly over-predicted lateral spreading displacements for this site. They concluded that the sand lenses were likely not horizontally continuous and that the strength of the clays between the liquefiable lenses must have been sufficient to limit ground deformations.

Lateral displacement indices (LDIs) were computed for the five CPT soundings using two different procedures and a sequence of refinements to evaluate their impacts on the results. One set of LDIs was computed using the liquefaction triggering correlation by Boulanger & Idriss (2015) with strains estimated using the procedures in Idriss & Boulanger (2008) based on Ishihara & Yoshimine (1992). The second set of LDIs was computed using the liquefaction triggering correlation by Robertson & Wride (1998) with the procedure by Zhang *et al*. (2004) to arrive at the lateral displacement (LD) values that might be expected for a point located about 6 m back from the canal edge. Both procedures were first applied using the common practice of point-by-point calculations without transition or thin-layer corrections and using

all applicable default parameters. The default parameters include using $I_c \leq 2.6$ for identification of sand-like (or liquefiable) soils and using $C_{FC} = 0$ for estimating FC in the Boulanger & Idriss (2015) liquefaction triggering procedure. The LDs ranged from 176 to 313 cm (median of 230 cm) and the LDIs ranged from 56 to 123 cm (median of 76 cm) for the five CPT soundings. The LDs are greater than the LDIs primarily because the Zhang *et al*. (2004) procedure includes a multiplier of 2.4 on displacements for the chosen point 6 m back from the canal edge. Regardless, the application of either procedure without transition or thin-layer corrections greatly over-predicts the potential for liquefaction effects at this site.

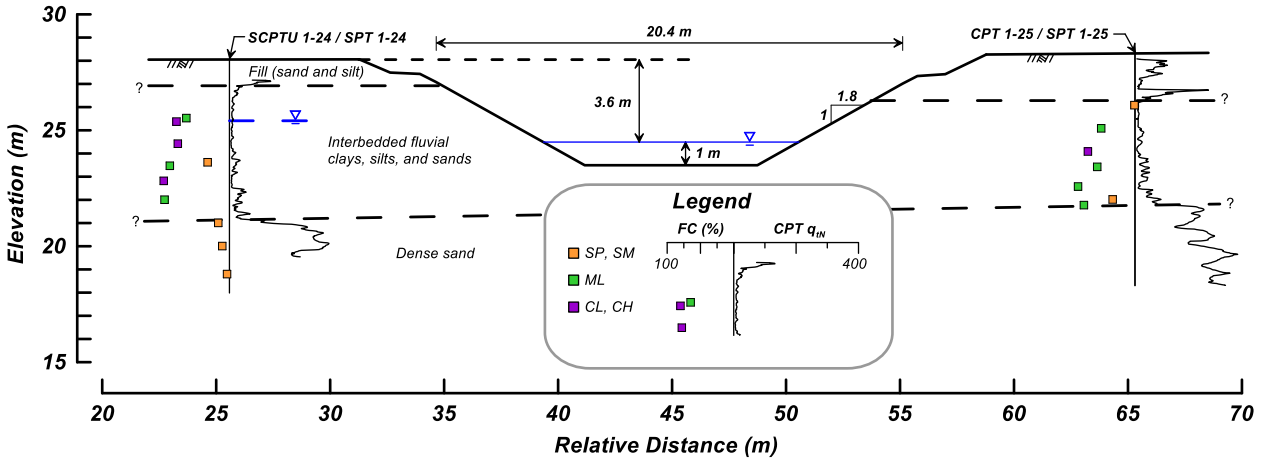

Figure 15: Cross-section of Çark Canal with CPT and borehole data near the channel (modified from Youd *et al*., 2009).

The LDI procedure using Boulanger & Idriss (2015) was then used to compute LDI values with the progressive addition of transition corrections, thin-layer corrections, and a site specific calibration to the FC data (i.e., the C_{FC} parameter). The median LDI for the five CPT soundings reduced to 67 cm with transition corrections, to 53 cm with transition and thin-layer corrections, and to 36 cm with both corrections and the site-specific C_{FC} calibration ($C_{FC} = 0.27$). The cumulative effect of these refinements are illustrated for CPT 1-23 in Figure 16, showing the cone tip resistance, factor of safety against liquefaction triggering, the maximum potential shear strain, and the integrated LDI profile for the first analysis case (no corrections; black lines) and last analysis case (all refinements combined; red lines). Each of the above refinements contributed to a progressive reduction in the estimated LDIs, but the last analysis case with all refinements combined still over-predicts the potential for liquefaction effects at this site.

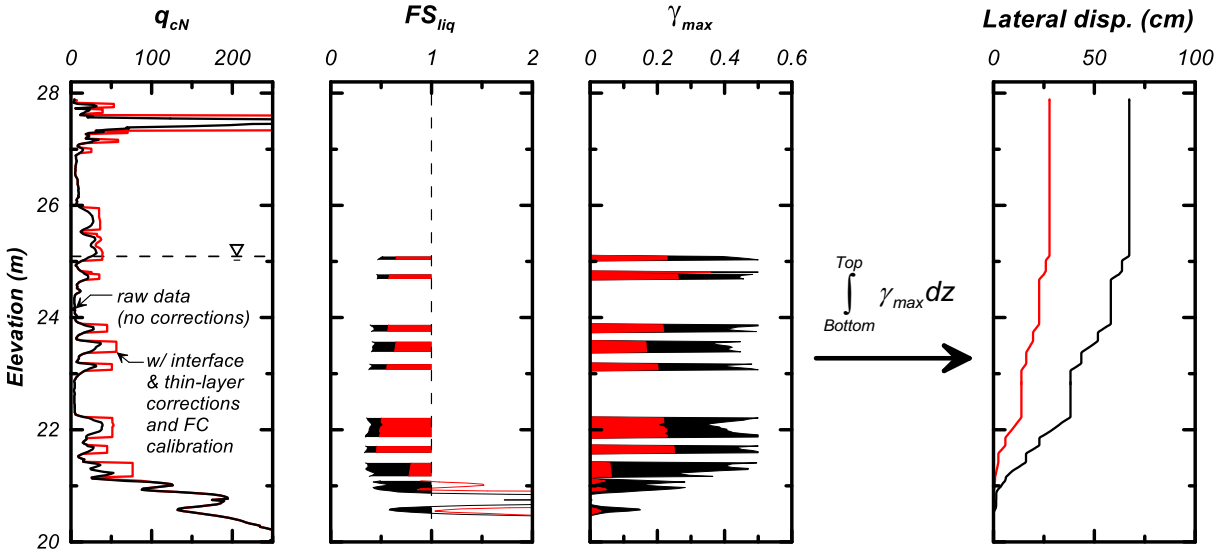

Figure 16: LDI results for CPT 1-23 without any adjustments (black lines) and with application of transition and thin-layer corrections and a site-specific fines content calibration (red lines).

The sensitivity of these LDI results to the I_c cutoff was also examined. If liquefiable soils are instead identified using $I_c \leq 2.4$, the median LDI is further reduced to 10 cm using both corrections and the revised site-specific C_{FC} value of 0.41. The site characterization data do not indicate that a lower I_c cutoff is justifiable for this site, but these sensitivity results

do illustrate the potential value in detailed site-specific field sampling and laboratory testing to refine the I_c cutoff used in these analyses.

NDAs of this site were performed using stochastic realizations of the interbedded sand and clay stratigraphy to assess the impact of spatial variability on the potential deformations. The realizations were produced using a transition probability geostatistical approach (Carle, 1999, Weissmann *et al*., 1999) with parameters determined from analysis of the CPT data, supplemented by estimates based on the depositional environment. Realizations conditional on the CPTs on either side of the canal were produced using different estimates for the horizontal mean lengths and percent sand-like materials in the critical stratum. The realization shown in Figure 17 is for a case with 40% sand with horizontal and vertical mean lengths for the sand lenses of 10 m and 26 cm, respectively.

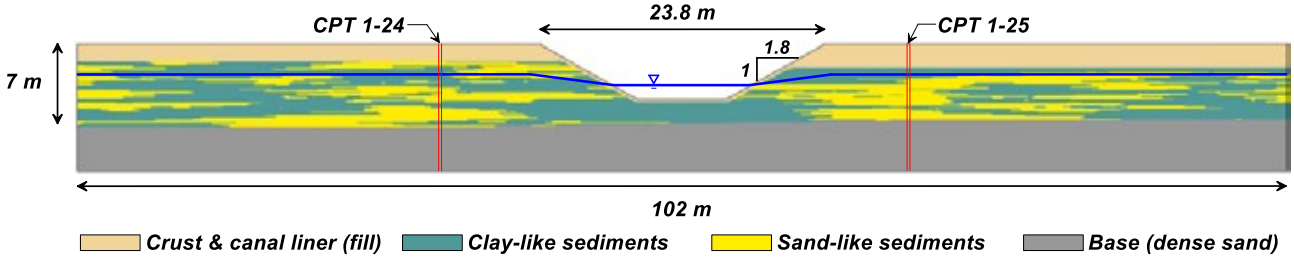

Figure 17: Realization B10-3 based on sand with sill = 40%, l_y = 10 m, and l_z = 0.26 m.

Representative properties for the sand and clay portions of the critical stratum were selected by binning the data for the sand-like and clay-like portions of the stratum and examining the data for spatial patterns separately. The sand-like materials were characterized using q_{c1Ncs} = 115 which is approximately the median value after applying transition and thin-layer corrections and the site-specific C_{FC} calibration. The clay-like materials were characterized using an undrained shear strength (s_u) of 50 kPa, which is approximately the median value based on an N_{kt} of 15. The fill layer and underlying dense sands layers were also characterized using median properties estimated from the CPT data.

The sand-like sediment in the critical stratum and underlying dense sand layer were modeled using the user-defined PM4Sand constitutive model (Boulanger & Ziotopoulou, 2015; Ziotopoulou & Boulanger, 2016). The constitutive model parameters were calibrated to the cyclic resistance ratios estimated from the CPT based liquefaction triggering correlation of Boulanger & Idriss (2015).

The clay-like sediment in the critical stratum and the overlying fill layer were modeled using the Mohr Coulomb constitutive model in FLAC.

The input motion was the E-W component of the recording from Sakarya scaled to a peak ground acceleration of 0.4 g. The motion was specified as an outcrop motion for the underlying dense sand. The base of the model was a compliant boundary and the opposing side boundaries were attached.

Contours of peak shear strain and lateral displacement after strong shaking are shown in Figure 18 for realization B10-3 (Figure 17). Shear strains in the sand lenses are greatest where the lenses are thickest and closest to the canal face, and smallest when the lenses are thinner and isolated. The banks of the canal have maximum lateral displacements of about 6 to 8 cm toward the canal for this realization. The results from other realizations gave maximum lateral displacements of about 2 to 10 cm depending on the parameters used to generate the realizations. Overall, the lateral displacements from the NDAs are in the range of what might reasonably have developed at this site without causing damage or cracking that would be visible during post-earthquake inspections.

Sensitivity analyses included examining the effect of uncertainty in the input ground motion on the LDI and NDA results. For example, reducing the peak ground acceleration to 0.3 g reduces the estimated ground displacements for both analysis methods, but the LDI results still significantly over-predict the potential for liquefaction effects at this site.

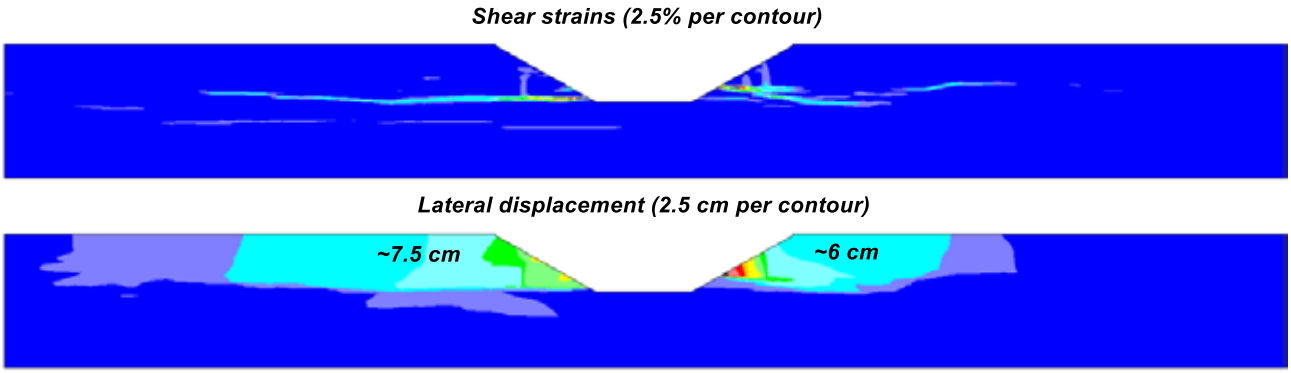

Figure 18: Contours of peak shear strain and lateral displacements toward the canal after earthquake shaking for realization B10-3.

These comparisons illustrate that the discontinuous nature of sand lenses in interbedded sand, silt and clay deposits can be an important factor influencing the potential for lateral spreading displacements. Simplified analysis procedures that assume horizontal continuity of sand lenses can be expected to over-predict liquefaction effects if the sand lenses are, in fact, not horizontally continuous over the length scale of potential deformation mechanisms. Improvements in our ability to account for these effects will require better guidance on geologic modelling, stochastic procedures, and site investigation practices. The results of this case study illustrate how several factors from Table 1 can contribute to over-prediction of liquefaction effects at a specific site. Analyses were able to predict the absence of significant ground deformations at this site only after the CPT soundings were corrected for transition and thin-layer effects, the spatial variability of the interbedded deposits was accounted for, and the analysis method was upgraded to a 2-D NDA. Stochastic realizations for representing spatial variability in NDAs offer the potential for significant insights on field behaviours, although they are not currently practicable for routine applications. Thus, future work is needed for providing guidance on how the effects of spatial variability can be incorporated into simplified analysis procedures.

6 CONCLUDING REMARKS

Case histories have shown that current liquefaction evaluation procedures and practices can have a tendency to over-predict liquefaction effects in interbedded sand, silt, and clay deposits. This tendency is attributed to several contributing factors as summarized in Table 1, with the importance of each factor depending on site-specific conditions and the analysis method employed.

The correction of CPT data for transition and thin-layer effects can be important for interbedded deposits. Incorporating these corrections reduced the degree to which 1-D LDIs over-predicted lateral spreading displacements at the Çark canal site and were important for the calibration of the constitutive model used in the NDAs. Additional work is needed to develop improved tools and guidance for applying these corrections in practice, including distinguishing between distinct interfaces (e.g., erosional contacts) and gradual transitions in soil characteristics (e.g., graded bedding).

The further development of CPT-based procedures for evaluating liquefaction or cyclic softening effects in intermediate soils is expected to benefit from mechanistic models for relating cone penetration and cyclic loading responses. The direct axisymmetric cone penetration model developed for use with the MIT-S1 constitutive model provides a means for relating cone penetration resistances to the constitutive properties of intermediate soils. The initial results obtained using laboratory-measured cyclic strengths with simulated cone penetration resistances for silt and clay mixtures suggest this approach is promising.

Re-examination of the performance of a site underlain by interbedded soils along the Çark canal in the 1999 M=7.5 Kocaeli earthquake illustrated how several factors can contribute to an over-prediction of liquefaction effects. Analyses were able to predict the absence of significant ground deformations at this site only after the CPT soundings were corrected for transition and thin-layer effects, the spatial variability of the interbedded deposits was accounted for, and the analysis approach was upgraded to a 2-D nonlinear deformation analysis. Other factors may have contributed to the good performance of this site during the Kocaeli earthquake, but their potential contributions are difficult to assess based on the existing data.

The advancement of liquefaction evaluation procedures for interbedded sand, silt and clay deposits will require a systematic examination of the various contributing factors listed in Table 1. The ability to address these factors will require improvements in experimental, theoretical and site characterization methods. Re-evaluation of case histories

involving interbedded deposits, with due consideration to all contributing factors, will be important for developing improved procedures and advancing practice.

7 ACKNOWLEDGMENTS

The authors appreciate the financial support of the National Science Foundation (awards CMMI-1300518 and 1547846), California Department of Water Resources (contract 4600009751), and California Division of Safety of Dams (contract 4600009523) for different aspects of the work described in the paper. Any opinions, findings, and conclusions or recommendations expressed in this material are those of the authors and do not necessarily reflect the views of either agency. The review of potential sources of bias in liquefaction evaluations for interbedded deposits benefited from discussions with Jonathan Bray, Brady Cox, Misko Cubrinovski, Kenneth Stokoe, Sjoerd van Ballegooy and others as part of collaborative studies examining sites in the Christchurch area. The review of fundamental aspects of relating cone penetrometer data to cyclic resistance ratios for different soil types draws from discussions with B. L. Kutter. Chris Krage helped prepare the stochastic realizations for Çark Canal and Ana Maria Parra Bastidas provided 1D limiting compression test data on the silt-kaolin mixtures for calibration of the MIT-S1 constitutive model. The research projects described herein have benefited from discussions with, and comments from, I. M. Idriss and B. L. Kutter. Additional comments on a draft of this paper were provided by Misko Cubrinovski and I. M. Idriss. The authors appreciate the above support and interactions.

8 REFERENCES

Beyzaei, C. Z., Bray, J. D., Cubrinovski, M., Riemer, M., Stringer, M. E., Jacka, M. & Wentz, F. J. (2015). Liquefaction resistance of silty soils at the Riccarton Road site, Christchurch, New Zealand. 6th International Conference on Earthquake Geotechnical Engineering, November 1 4, Christchurch, New Zealand.

Boulanger, R. W. & Idriss, I. M. (2007). Evaluation of cyclic softening in silts and clays. Journal of Geotechnical and Geoenvironmental Engineering, ASCE, 133(6), 641-652.

Boulanger, R. W. & Idriss, I. M. (2015). CPT-based liquefaction triggering procedure. Journal of Geotechnical and Geoenvironmental Engineering, ASCE, 142(2): 04015065, 10.1061/(ASCE)GT.1943-5606.0001388.

Boulanger, R. W., Kamai, R., & Ziotopoulou, K. (2014). Liquefaction induced strength loss and deformation: Simulation and design. Bulletin of Earthquake Engineering, Springer, 12: 1107-1128, 10.1007/s10518-013-9549-x.

Boulanger, R. W. & Ziotopoulou, K. (2015). PM4Sand (Version 3): A sand plasticity model for earthquake engineering applications. Report No. UCD/CGM-15/01. Center for Geotechnical Modeling, Department of Civil and Environmental Engineering, University of California, Davis, CA.

Canou, J. (1989). Piezocone et liquefaction des sables. Rapport de synthese des travaux realizes au CERMES, Research Report CERMES/ENPC, Paris, 176 p.

Carle, S. F. (1999. T-PROGS: Transition probability geostatistical software. University of California, Davis, CA.

Carraro, J. A. H., Bandini, P. & Salgado, R. (2003). Liquefaction resistance of clean and nonplastic silty sands based on cone penetration resistance. J. Geotechnical and Geoenvironmental Engineering, 129(11), 965-976.

Chai, J., Sheng, D., Carter, J.P. & Zhu, H. (2012). Coefficient of consolidation from non-standard piezocone dissipation curves. Computers and Geotechnics 41: 13-22.

Chu, D. B., Stewart, J. P., Boulanger, R. W. & Lin, P. S. (2008). Cyclic softening of low-plasticity clay and its effect on seismic foundation performance. Journal of Geotechnical and Geoenvironmental Engineering, ASCE, 134(11), 1595-1608.

Chu, D. B., Stewart, J. P., Youd, T. L. & Chu, B. L. (2007). Liquefaction-induced lateral spreading in near-fault regions during the 1999 Chi-Chi, Taiwan Earthquake. J. Geotechnical and Geoenvironmental Engineering, ASCE, 132(12), 1549-1565.

Colella, P. (1990). Multidimensional upwind methods for hyperbolic conservation laws. Journal of Computational Physics, 87: 171-200.

Cubrinovski, M., Rees, S. & Bowman, E. (2010. Effects of non-plastic fines on liquefaction resistance of sandy soils. 17, 125-144.

Cubrinovski, M. & Robinson, K. (2015). Lateral spreading: evidence and interpretation from the 2010-11 Christchurch earthquakes. 6th International Conference on Earthquake Geotechnical Engineering, November 1 4, Christchurch, New Zealand.

DeJong, J. T. & Randolph, M. (2012). Influence of partial consolidation during cone penetration on estimated soil behavior type and pore pressure dissipation measurements. JGGE, ASCE, 138(7), 777-788.

DeJong, J. T., Jaeger, R. A., Randolph, M. F., Boulanger, R. W., & Wahl, D. (2012). Variable penetration rate cone testing for characterization of intermediate soils. Geotechnical and Geophysical Site Characterization 4 (ISC'4), Coutinho and Mayne, eds., Taylor and Francis Group, London, 25-42.

Foray, P. & Pautre, J-L. (1988). Piezocone et liquefaction des sables: synthese des essais sur sites en Nouvelle-Zelande et des essais en Chambre de Calibration a l'IMG, Research Report, IMG, Grenoble, 70 p.

Frost, J. D., DeJong, J. T. & Saussus, D. R. (2006). Analytical investigation of friction sleeve length effects on stratigraphic interpretation. Intl. J. of Geomechanics, 6(1), 11-29.

GeoLogismiki (2016). CLiq v.2.0 – CPT liquefaction software. http://www.geologismiki.gr/products/cliq/, accessed 7/2016.

Huang, W., Sheng, D., Sloan, S.W. & Yu, H.S. (2004). Finite element analysis of cone penetration in cohesionless soil. Computers and Geotechnics, 31:517-528.

Idriss, I. M. & Boulanger, R. W. (2008). Soil liquefaction during earthquakes. Earthquake Engineering Research Institute.

Ishihara K. (1985). 'Stability of natural deposits during earthquakes.' Proceedings, 11th International Conference on Soil Mechanics and Foundation Engineering, San Francisco. Vol. 1, p. 321-376.

Ishihara, K. & Yoshimine, M., (1992). Evaluation of settlements in sand deposits following liquefaction during earthquakes. Soils and Foundations 32, 173–188.

Itasca (2011). FLAC, Fast Lagrangian Analysis of Continua, User's Guide, Version 7.0. Itasca Consulting Group, Inc., Minneapolis, MN.

Jaeger, R.A. (2012). Numerical and experimental study of cone penetration in sands and intermediate soils. Doctoral Dissertation, University of California, Davis.

Kokusho, T. (2003). Current state of research on flow failure considering void redistribution in liquefied deposits. Soil Dynamics and Earthquake Engineering, 23(7):585–603.

Kokusho, T., Ito, F., Nagao, Y. & Green, A. R. (2012). Influence of non/low-plastic fines and associated aging effects on liquefaction resistance. J. Geotechnical and Geoenvironmental Engineering, 138(6), 747-756.

Ladd, C.C. & Varallyay, J. (1965). The influence of stress system on the behavior of saturated clays during undrained shear. No. RR-R65-11. Massachusetts Institute of Technology Cambridge Soil Mechanics Division.

Landon, M.M. (2007). Development of a non-destructive sample quality assessment method for soft clays. Doctoral Dissertation, University of Massachusetts, Amherst.

LeBlanc, C., and Randolph, M. F. (2008). Interpretation of piezocones in silt, using cavity expansion and critical state methods. Proc. 12th International Conference of IACMAG, 822-829.

Liyanapathirana, D.S. (2009). Arbitrary Lagrangian Eulerian based finite element analysis of cone penetration in soft clay. Computers and Geotechnics 36: 851-860.

Mahmoodzadeh, H., Randolph, M.F. & Wang, D. (2014). Numerical simulation of piezocone dissipation test in clays. Geotechnique 64(8): 657-666.

Mayne, P. (2007). Cone Penetration Testing – A synthesis of highway practice. NCHRP Synthesis 268, Transportation Research Board, Washington, D.C.

Mo, P.Q., Marshall, A. M., & Yu, H.S. (2013). Centrifuge modeling of CPT in layered soils. Geotechnical and Geophysical Site Characterization 4 – Coutinho and Mayne (eds), Taylor and Francis Group, 219-225.

Mo, P.-Q., Marshall, A. M., & Yu, H.S. (2015). Centrifuge modelling of cone penetration tests in layered soils. Géotechnique 65, No. 6, 468–481.

Moss, R., Seed, R., Kayen, R., Stewart, J., Der Kiureghian, A. & Cetin, K. (2006). CPT-based probabilistic and deterministic assessment of in situ seismic soil liquefaction potential. Journal of Geotechnical and Geoenvironmental Engineering, 132(8), pp.1032-1051.

Moug, D. M., Boulanger, R. W., DeJong, J. T. & Jaeger, R. W. (2016). Simulation of cone penetration in anisotropic clay. Proc., GeoVancouver 2016, Canadian Geotechnical Society, Vancouver, Oct. 2-5.

Munter, S. K., Krage, C. P., Boulanger, R. W., DeJong, J. T. & Montgomery, J. (2016). Potential for liquefaction-induced lateral spreading in interbedded deposits considering spatial variability. Proceedings, Geotechnical and Structural Engineering Congress, Phoenix, AZ, Feb. 14-17, ASCE.

Nichols, G. (2009). Sedimentology and stratigraphy. Second edition, Wiley-Blackwell, John Wiley & Sons Ltd., West Sussex, UK.

Olson, S. M. & Johnson, C. I. (2008). Analyzing liquefaction-induced lateral spreads using strength ratios. J. Geotechnical and Geoenvironmental Engineering, ASCE, 134(8), 1035-1049.

Park, S.-S. & Kim, Y.-S. (2013). Liquefaction resistance of sands containing plastic fines with different plasticity. Journal of Geotechnical and Geoenvironmental Engineering, 139(5), 825-830.

Pestana, J.M. and Whittle, A. J. (1999). Formulation of a unified constitutive model for clays and sands. International Journal for Numerical and Analytical Methods in Geomechanics, 23: 125-1243.

Pestana, J.M., Whittle, A.J. & Gens, A. (2002). Evaluation of a constitutive model for clays and sands: Part II – Clay behaviour. International Journal for Numerical and Analytical Methods in Geomechanics, 26:1123-1146.

Price, A. B., Boulanger, R. W., DeJong, J. T., Parra Bastidas, A. M. & Moug, D. (2015). Cyclic strengths and simulated CPT penetration resistances in intermediate soils. 6th International Conference on Earthquake Geotechnical Engineering, November 1 4, Christchurch, New Zealand.

Robertson, P.K. (1990). Soil classification using the cone penetration test, Canadian Geotechnical J. 27(1), 151–58.

Robertson, P. K. (2009). Discussion of "Evaluation of Cyclic Softening in Silts and Clays" by Ross W. Boulanger and I. M. Idriss. J. Geotechnical and Geoenvironmental Engineering, 135:2(306), 306-307.

Robertson, P. K. & Fear, C. E. (1995). ''Liquefaction of sands and its evaluation.'' Proc., 1st Int. Conf. on Earthquake Geotechnical Engineering.

Robertson, P. & Wride, C., (1998). Evaluating cyclic liquefaction potential using the cone penetration test. Canadian Geotechnical Journal, 35(3), pp.442--459.

Salgado, R., Mitchell, J. K. & Jamiolkowski, M. (1997). Cavity expansion and penetration resistance in sand. Journal of Geotechnical and Geoenvironmental Engineering, 123(4), 344-354.

Silva, M. F., & Bolton, M. D. (2004). Centrifuge penetration tests in saturated layered sands. Proc. ISC-2 on Geotechnical and Geophysical Site Characterization, Viana da Fonseca and Mayne (eds), 377-384.

Stringer, M., Beyzaei, C., Cubrinovski, M., Bray, J. D., Riemer, M., Jacka, M. & Wentz, F. (2015). Liquefaction characteristics of Christchurch silty soils: Gainsborough Reserve. 6th International Conference on Earthquake Geotechnical Engineering, November 1 4, Christchurch, New Zealand.

Van Ballegooy, S., Malan, P., Lacrosse, V., Jacka, M. E., Cubrinovski, M., Bray, J. D., O'Rourke, T. D. O., Crawford, S. A. & Cowan, H. (2014). Assessment of liquefaction-induced land damage for residential Christchurch. Earthquake Spectra, EERI, 30(1), 31-55.

Van Ballegooy, S., Wentz, F. & Boulanger, R. W. (2015). Evaluation of CPT-based liquefaction procedures at regional scale. Soil Dynamics and Earthquake Engineering, 10.1016/j.soildyn.2015.09.016.

Van den Berg, P., deBorst, R. & Huetink, H. (1996). An Eulerian finite element model for penetration in layered soil. International Journal for Numerical and Analytical Methods in Geomechanics, 20(12): 865–86.

Vreugdenhil, R., Davis, R. & Berrill, J. (1994). Interpretation of cone penetration results in multilayered soils. Intl. J. Numerical and Analytical Methods in Geomechanics, 18: 585-599.

Walker, J. & Yu, H.S. (2006). Adaptive finite element analysis of cone penetration in clay. Acta Geotechnica 1: 43-57.

Walker, J. and Yu, H.S. (2010). Analysis of the cone penetration test in layered clay. Geotechnique, 60(12): 939-948.

Wang, D., Bienen, B., Nazem, M., Tian, Y., Zheng, J., Pucker, T., Randolph, M.F. (2015). Large deformation finite element analysis in geotechnical engineering. Computers and Geotechnics 65: 104-114.

Weissmann, G. S., Carle, S. F. & Fogg, G. E. (1999). Three-dimensional hydrofacies modeling based on soil surveys and transition probability geostatistics. Water Resources Research, 35(6), 1761-1770.

Yi, J.T., Goh, S.H., Lee, F.H. & Randolph, M.F. (2012). A numerical study of cone penetration in fine-grained soils allowing for consolidation effects. Geotechnique 62(8): 707-719.

Youd, T. L., Cetin, K. O., Bray, J. D., Seed, R. B., Durgunoglu, H. T. & Onalp, A. (2000). Geotechnical site investigation at lateral spread sites. http://peer.berkeley.edu/publications/_turkey/adapazari/index.html, last accessed 7/2016.

Youd, T. L., DeDen, D. W., Bray, J. D., Sancio, R., Cetin, K. O. & Gerber, T. M. (2009). Zero-displacement lateral spreads, 1999 Kocaeli, Turkey, earthquake. Journal of Geotechnical and Geoenvironmental engineering, 135(1), 46-61.

Youd, T. L., Hansen, C. M. & Bartlett, S. F. (2002). Revised multilinear regression equations for prediction of lateral spread displacement. Journal of Geotechnical and Geoenvironmental Engineering, 128(12), 1007-1017.

Youd, T. L., Idriss, I. M., Andrus, R. D., Arango, I., Castro, G., Christian, J. T., Dobry, R., Finn, W. D. L., Harder, L. F., Hynes, M. E., Ishihara, K., Koester, J. P., Liao, S. S. C., Marcuson, W. F., Martin, G. R., Mitchell, J. K., Moriwaki, Y., Power, M. S., Robertson, P. K., Seed, R. B. & Stokoe, K. H. (2001). Liquefaction resistance of soils: summary report from the 1996 NCEER and 1998 NCEER/NSF workshops on evaluation of liquefaction resistance of soils. Journal of Geotechnical and Geoenvironmental Engineering, American Society of Civil Engineers, 127(10): 817-833.

Yu, H. S., Herrmann, L. R., & Boulanger, R. W. (2000). Analysis of steady cone penetration in clay. Journal of Geotechnical and Geoenvironmental Engineering, ASCE, 126(7), 594-605.

Zhang, G., Robertson, P. K. & Brachman, R. W. I. (2004). Estimating liquefaction-induced lateral displacements using the standard penetration test or cone penetration test. Journal of Geotechnical and Geoenvironmental Engineering, 130(8), 861-871.

Ziotopoulou , K. & Boulanger, R. W. (2016). Plasticity modeling of liquefaction effects under sloping ground and irregular cyclic loading conditions. Soil Dynamics and Earthquake Engineering, 84 (2016), 269-283.